Spectral Analysis and Filtering Techniques in Digital Spatial Data Processing

Jeng-Jong Pan
TGS Technology, Inc., EROS Data Center, U. S. Geological Survey, Sioux Falls, SD 57198

ABSTRACT: A filter toolbox has been developed at the EROS Data Center, U.S. Geological Survey, for retrieving or removing specified frequency information from two-dimensional digital spatial data. This filter toolbox provides capabilities to compute the power spectrum of a given data and to design various filters in the frequency domain to filter the data. The power spectrum can be used to identify the frequencies of periodic noises to assist in the design of suitable filters to remove noise from the data. Three types of filters are available in the toolbox: point filter, line filter, and area filter. Both the point and line filters employ Gaussian-type notch filters, and the area filter includes the capabilities to perform high-pass, band-pass, low-pass, and wedge filtering techniques. These filters are applied for analyzing satellite multispectral scanner data, airborne visible and infrared imaging spectrometer (AVIRIS) data, gravity data, and the digital elevation models (DEM) data. This filter toolbox can also be widely applied to other digital spatial data represented as gridded format.

INTRODUCTION

THE ANALYSIS OF DIGITAL SPATIAL DATA sometimes requires the retrieval of information or the removal of noise from the data so that subsequent data analysis can be performed with a high reliability. A filter toolbox has been developed at the EROS Data Center, U. S. Geological Survey, to provide this capability. This filter toolbox, written in FORTRAN, provides capabilities to compute the power spectrum of the data and to design filters in the frequency domain that can be used to filter the data.

The applications of frequency analysis to one-dimensional digital elevation observations and two-dimensional image data have been discussed by Moik (1980), Chen *et al*. (1987), and Hassan (1988). In the frequency domain, some important information can be obtained from the analysis of power spectrum. For example, in the analysis of potential field data (gravity and magnetic data), the average depth to an ensemble of source bodies is proportional to the slope of the logarithm of the power spectrum (Spector and Grant, 1970). For remotely sensed data processing, the power spectrum can be used to identify the frequencies of periodic noises resulting from the variations between sensors in the imaging system or from other factors (Moik, 1980). The quantifiable characteristics of spatial data derived from the analysis of their power spectra provide useful information for the design of suitable filters to accomplish research requirements.

In the toolbox filters are generally referred to as point filter, line filter, and area filter. The point filter, equivalent to the Gaussian notch filter, can be used to remove noise-related spikes in the frequency domain. The line filter is useful in removing line-type noise-related frequency responses that occur in some multispectral imaging systems. Area filters include high-pass, band-pass, low-pass, and wedge filters which are useful for analysis of potential field data, digital elevation models (DEM), remotely sensed data, and other types of spatial data.

SPECTRAL ANALYSIS

The Fourier transform provides an analytic approach to converting data from the spatial domain to the frequency domain. Transformation of a given spatial data into the frequency domain involves conversions of data from spatial coordinates to frequency coordinates. Spectral analysis is an approach to analyzing the Fourier transformed spatial data in the frequency domain.

For an M by N spatial data $f(m\Delta d, n\Delta d)$, where m and n are the indexes in the x and y spatial coordinates, respectively, $m=0,1,\ldots,M-1$, and $n=0,1,\ldots,N-1$; Δd is the sampling interval. The transformed spatial data $H(u,v)$, where u and v are frequency coordinates, can be obtained by the discrete Fourier transform (Oppenheim and Schafer, 1975): that is,

$$F(u,v) = \frac{1}{M\,N} \sum_{n=0}^{N-1} \sum_{m=0}^{M-1} f(m,\, n)\mathrm{e}^{-i2\pi(\frac{mu}{M}+\frac{nv}{N})}$$

where $i=\sqrt{-1}$. The inverse Fourier transform is

$$F(m,\, n) = \sum_{n=0}^{N-1} \sum_{m=0}^{M-1} F(u,\, v)\mathrm{e}^{i2\pi(\frac{mu}{M}+\frac{nv}{N})}$$

Cooley and Turkey (1965) have developed a fast Fourier transform (FFT) algorithm to improve the speed of the above computation.

In general, the transformed data $F(u,v)$ is a complex quantity with the real part $R(u,v)$ and the imaginary part $I(u,v)$,

$$\begin{aligned} F(u,\, v) &= R(u,v) + iI(u,\, v) \\ &= |\, F(u,\, v)\,|\, \mathrm{e}^{i\phi} \end{aligned}$$

where

$$|\, F(u,v)\,| = \sqrt{R(u,\, v)^2 + I(u,\, v)^2}$$

is the amplitude and

$$\phi = \tan^{-1} \frac{I(u,\, v)}{R(u,\, v)}$$

is the phase in the frequency domain.

Because the spatial data are real values, then $R(u,v)$ is even and $I(u,v)$ is odd; that also makes the amplitude even and the phase odd. Amplitude represents the distribution of magnitude of various frequency (or wavelength) components, and the phase contains the information of position of these frequency components.

The power spectrum $P(u,v)$, $P(u,v)=|\,F(u,v)\,|^2$, shows the power density versus frequency relationship. The power spectrum can be utilized to analyze the frequency components of input spatial data. Usually, $P(u,v)$ is displayed in dB, where

$$P(u,\, v) \text{ in } dB = 20 \log_{10} |\, F(u,v)\,|$$

so that the small variation in the power spectrum can be amplified.

PHOTOGRAMMETRIC ENGINEERING AND REMOTE SENSING,
Vol. 55, No. 8, August 1989, pp. 1203–1207.

0099-1112/89/5508–1203$02.25/0

FILTERING TECHNIQUES

The objective of the filtering techniques mentioned in this paper is to retrieve or remove specified frequencies in the frequency domain. The filter is multiplied with the transformed spatial data $F(u,v)$ and the result is transformed back into the spatial domain. In the toolbox, the desired filters can be designed to manipulate points, lines, and regions in the frequency domain.

The point filter is used to remove points that are related to periodic noises in the frequency domain. Theoretically, periodic or almost periodic noises appear as delta functions in the power spectrum (Bendat and Piersol, 1971). The form of a point filter, the same as a Gaussian notch filter, is defined as

$$H(u,\ v) = 1.0 - e^{-\frac{r2}{2\sigma 2}}$$

where $r=\sqrt{\sqrt{(u-u')^2 + (v-v')^2}}$, (u',v') is the point that will be removed, and σ is the standard deviation of the Gaussian distribution.

The line filter is used to remove line-type frequency distributions which are related to the coherent noises that occur in some of multispectral imaging systems (Bailey *et al.*, 1988). The form of the line filter, an extension of the point filter, is defined as

$$H(u,\ v) = 1.0 - e^{-\frac{r2}{2\sigma 2}}$$

where $r=|u-u'|$ (or $r=|v-v'|$), u' (or v') is the line that will be removed, and σ is the standard deviation of the Gaussian distribution.

The area filters include the high-pass, band-pass, low-pass, and wedge filters. The general form of these filters is

$$H(u,\ v) = H(r,\theta) = \begin{cases} 1 & r_1 \le r \le r_2,\ \theta_1 \le \theta \le \theta_2 \\ 0 & \text{otherwise} \end{cases}$$

where $r=\sqrt{u^2+v^2}$, and $\theta=\tan^{-1}(v/u)$. The range of r is from 0 to the Nyquist frequency f_N, $f_N = 1/2\Delta d$, where Δd is the sampling interval, and the angle θ is from $-90°$ to $90°$. In sampling theory, the sampling interval cannot be greater than the one-half the smallest wavelength within the spatial data (Bath, 1974).

The high-pass filter passes only those frequencies above a specified cutoff frequency and is useful for extracting high frequency features from spatial data. On the opposite side, the low-pass filter only passes frequencies less than a specified cutoff frequency, that covers the origin $H(0,0)$, so the mean and low frequency features of input data are preserved in the filtered data. The band-pass filter passes frequency responses between two cutoff frequencies and is a combination of low- and high-pass filters. The wedge filter (also called strike or directional filter) is used to extract the spatial features along a direction in a specified angle range. The extracted spatial features are perpendicular to the specified frequency direction.

The area filters mentioned above are ideal filters. The discontinuities in an ideal filter result from truncation at the cutoff frequencies which produce ripple-like Gibb's phenomena (Oppenheim and Schafer, 1975). The Gibb's phenomena can be reduced by multiplying a proper window to the ideal filter. Four windows are available in the filter toolbox for area filters: Bartlett, Hanning, Hamming, and Blackman windows. They are defined as (Oppenheim and Schafer, 1975)

Bartlett (triangular) window:

$$W(r) = 1 - |r|/r_0 \qquad |r| \le r_0$$

Hanning window:

$$W(r) = 0.5 + 0.5\cos(2\pi r/r_0) \qquad |r| \le r_0$$

Hamming window:

$$W(r) = 0.54 + 0.46\cos(2\pi r/r_0) \qquad |r| \le r_0$$

Blackman window:

$$W(r) = 0.42 + 0.5\cos(2\pi r/r_0) + 0.08\cos(4\pi r/r_0) \qquad |r| \le r_0$$

where r_o is the width of the filter and $r = \sqrt{u^2 + v^2}$. $W(r)$ is zero if $|r| > r_o$.

There is no straight-forward procedure to derive the best width for each window. Experimental tests showed that the width of the window is more important than the type of window used. The width of the window should be of the same order as the smallest wavelength of interest in the spectral analysis (Bath, 1974).

The filter design procedure using a window starts by designing an ideal filter in the frequency domain, then transforms this filter to the spatial domain, and multiplies with a proper window, then transfers the windowed filter back to the frequency domain. The filter technique discussed in this paper deals only with amplitude response modification; the phase is preserved as the original input data because the locations of spatial features will not be varied.

APPLICATIONS

POINT FILTER

The point filter can be used to remove periodic noises, such as the striping which occurs in multispectral scanner data. Striping could be caused by a variety of mechanisms, such as sensor gain and offset variations, data outages, and tape recorder dropouts (Moik, 1980).

Figure 1(a) shows a striping problem occurred in a 512 by 512

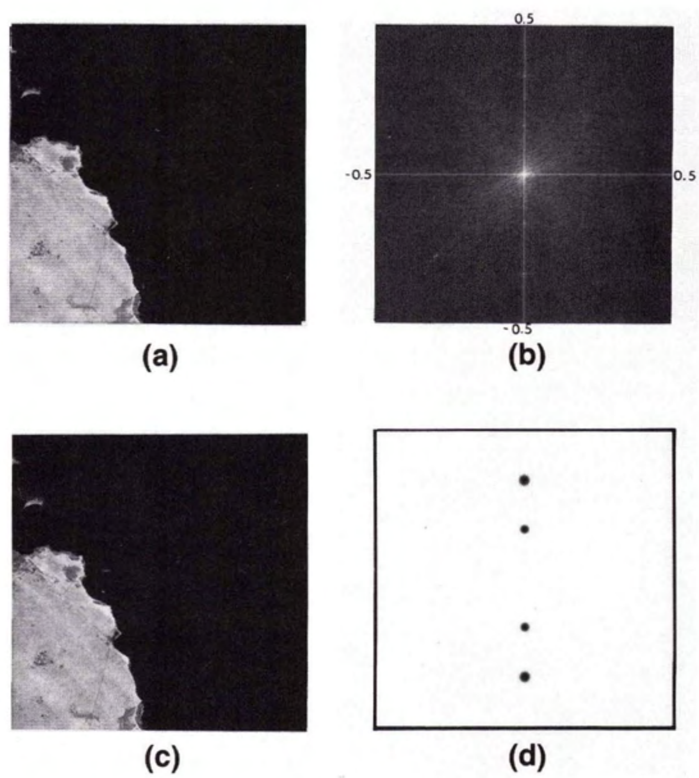

FIG. 1. (a) A multispectral scanner (MSS) image with striping. (b) The corresponding power spectrum. (c) The filtered image. (d) The point filter used for destriping.

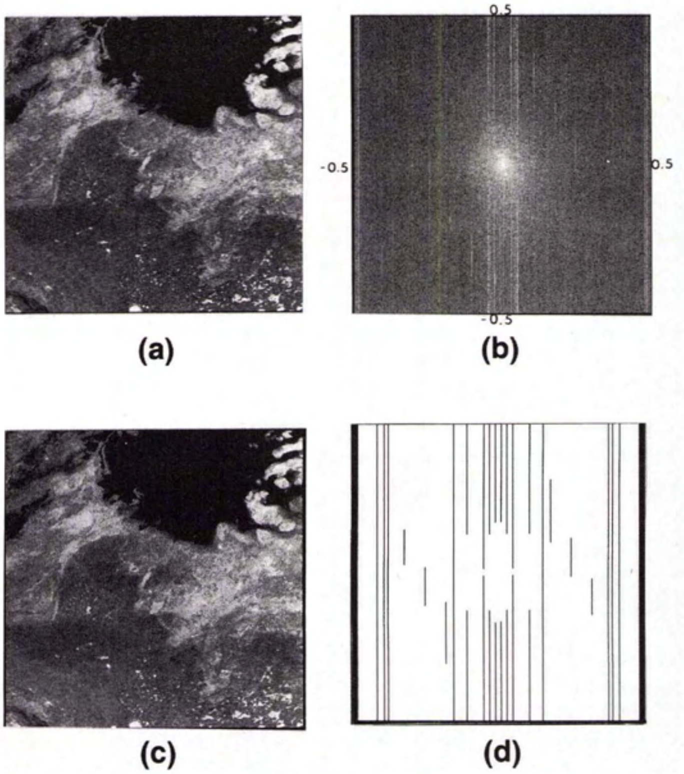

FIG. 2. (a) Single band AVIRIS image centered at wavelength 2220 nm. (b) The corresponding power spectrum. (c) The filtered image. (d) The line filter used for noise removal.

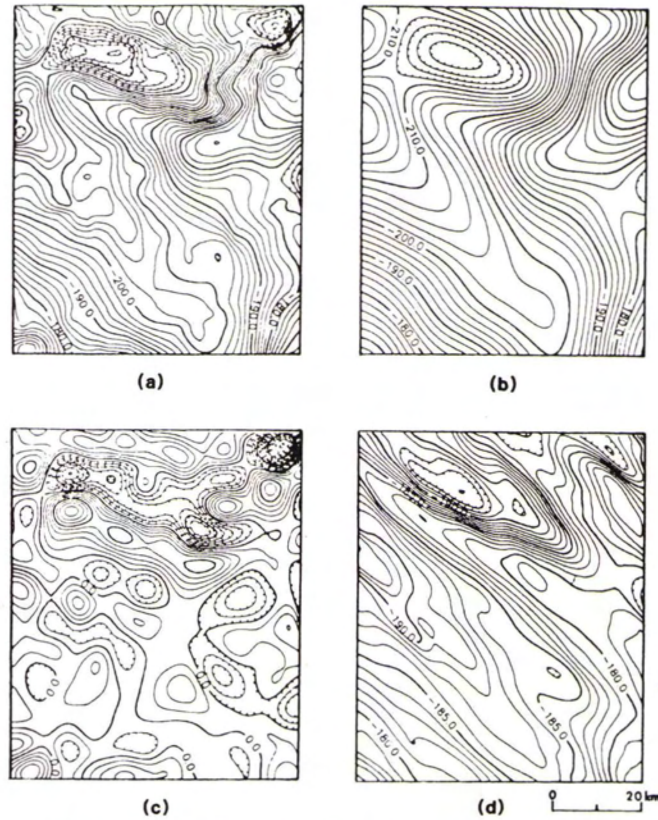

FIG. 3. (a) Demonstration gravity data. (b) Low-pass filtered map showing wavelengths greater than 20 km. (c) Band-pass filtered map showing wavelengths between 8 to 20 km. (d) Northwest wedge filtered map.

pixels Landsat multispectral scanner (MSS) image. The striping is significant on the land part of the image, but is hard to see in the ocean section. However, it may be more detectable after the image is enhanced.

Figure 1(b) is the power spectrum of Figure 1(a). There are two peaks on the upper central vertical line, where $u = 0$, since the striping is horizontally manifested by periodic noises. The two corresponding peaks in the lower part of the power spectrum are symmetric to the upper two peaks because the power spectrum is an even function. These two peaks at frequencies of 1/6 and 1/3 cycle/line are related to the six detectors of the scanner.

The peaks that appear in the power spectrum might be confused with narrow-band signal information. In practical processing, the separation of any noise from the data is dependent on knowledge about the original true data. Using the point filter to remove noise-related peaks could cause errors in the filtered data. In most cases, these errors could be too small to be identified by the human eye.

Figure 1(c) is the filtered image where most of the striping has been removed; Figure 1(d) is the point filter designed to remove the noise-related frequencies. A minor striping left around the image edges, called edge effects, could be reduced either by expanding the input data size, then truncating the expanded edges after filtering, or by multiplying a suitable window to the input data before filtering to suppress the discontinuities around the edges.

LINE FILTER

Line-type noise-related frequencies can be identified in some airborne visible and infrared imaging spectrometer (AVIRIS) and thermal infrared multispectral scanner (TIMS) data. AVIRIS and TIMS, useful geological remote sensing tools, provide geologists with capabilities to determine lithologic variation and rock composition, and to measure physical parameters (for example, temperature and percent reflectance) on the Earth's surface.

From the results of a preliminary study (Bailey *et al.*, 1988), it was found that an AVIRIS image was contaminated by a variety of coherent noises. Figure 2(a) shows an AVIRIS image with a wavelength centered at 2220 nm and Figure 2(b) is the corresponding power spectrum. All components of the coherent noises occured at several horizontal frequencies (u-axis) with different range in vertical frequencies (v-axis). These linear noise-related frequencies can be removed by using a line filter.

Figure 2(c) is the filtered image and Figure 2(d) is the line filter designed to remove some identifiable line-type frequencies. As discussed earlier, the precise removal of all coherent noises is dependent on the users knowledge of the original image.

AREA FILTERS

Area filters may serve a number of purposes in processing various types of digital spatial data. Two examples, gravity and DEM data processing, will be discussed here. For the purposes of the following discussion, use of the term wavelength is substituted for the term frequency used in earlier discussions. As a rule, wavelength is inversely proportional to the frequency.

Gravity data measured at or above the Earth's surface contain information about buried source bodies. A principal purpose for obtaining gravity data is to locate and determine distributions of these source bodies. Figure 3(a) shows a test gravity map and Figures 3(b), 3(c), and 3(d) show the derivative products from Figure 3(a).

In order to study local and shallow source bodies, the regional

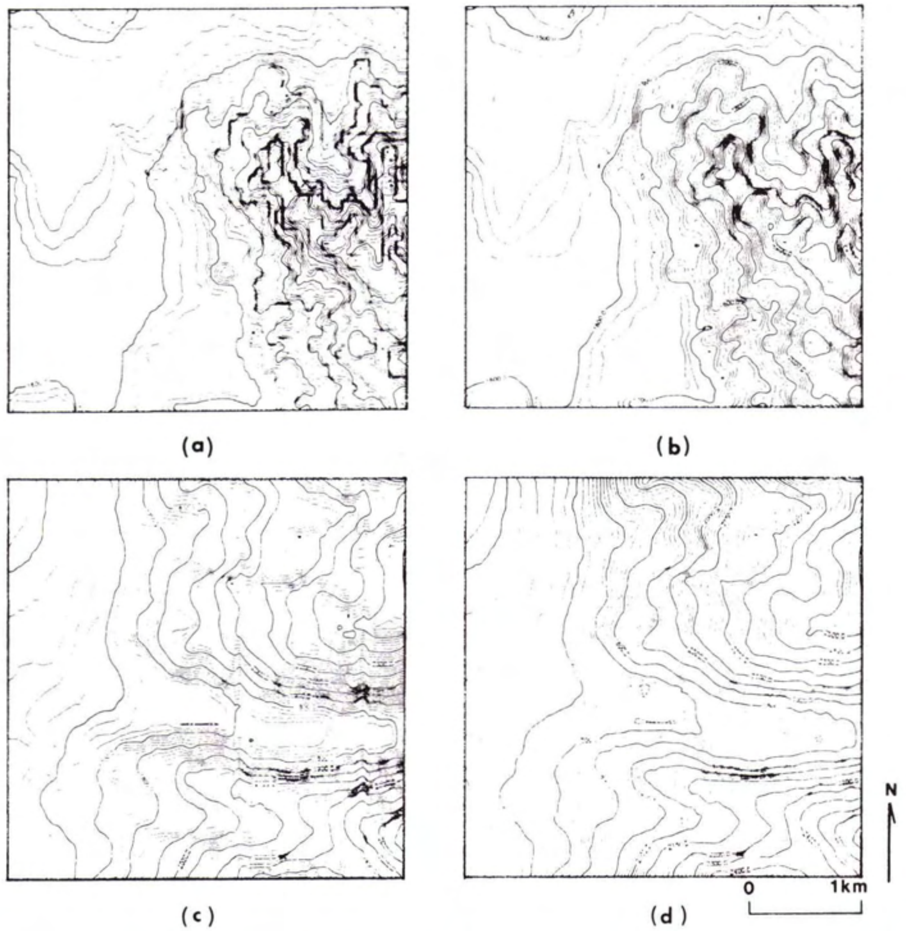

FIG. 4. Contour maps of DEM data. (a) DEM dataset near Ft. Huachuca, Arizona. (b) Low-pass filtered map of (a). (c) DEM dataset near Salt Lake City, Utah. (d) Low-pass filtered map of (c).

gravity related to the deep structures (e.g., the basement) should be removed before further quantitative modeling. The regional gravity is a representation of major geological features which are not directly expressed on the Earth's surface. The regional gravity contain long wavelength features which can be used to interpret structural trends over a large area.

Figure 3(b) shows the result of using a low-pass filter to extract regional gravity, where only the signals with wavelengths greater than 20 km are passed. The wavelength selected here is for demonstration purposes only. The actual wavelength can be determined either by the specific objectives of the study or by estimation from the power spectrum (Spector and Grant, 1970). Because the average depth to the source bodies is, as a rule of thumb, half of the wavelength, the low-pass filtering approach to compute the regional gravity is more quantitative than using a high order polynomial function to estimate the regional gravity.

Figure 3(c) shows a band-pass filtered map with wavelengths from 8 to 20 km. It can be used to study local structures that have been separated from deep parts. Figure 3(d) is a wedge filtered map. Only gravity data along the northwest direction is preserved, which is helpful to determine the strike of faults and delineate trends of geological features.

Because gravity is a potential function (Dehlinger, 1978), which obeys Newton's universal law of gravity, the gravity value is inversely proportional to the square of the distance between of the survey station and the source body. This results in the contour lines of a gravity map smoother than contours from other digital spatial data. In contrast to the rapid change of digital numbers between pixels, which may produce discontinuities in most imagery data, the variation of gravity value is more gradual. Consequently, there are no visible "ringing" effects in filtered gravity data.

Digital elevation models (DEM) data are very useful for geophysical data reduction, geomorphometrical interpretation, drainage network study, and various manipulations within a geographic information system The scale of DEM data discussed here is 1:24,000 with a 30-metre sampling interval. The accuracy of DEM data is dependent on the quality of the collected data and the subsequent resampling algorithms. Some DEM data have embedded random noises that are caused by observational errors. These noises could inhibit feature extraction and impede further data interpretation.

Noise-patterns in contaminated DEM data may appear as vertical lines, horizontal lines, or both. These patterns are more visible when the DEM data are converted to contour maps or shaded-relief images. Figure 4(a) shows a contour map of a DEM dataset near Ft. Huachuca, Arizona. Some rectangular-like noise patterns have biased the real topographic features. A low-pass filter was designed to remove the wavelengths less than 120 metres, which is estimated from the contour map. Figure 4(b) is the filtered contour map, where the noise patterns have been significantly reduced.

Figure 4(c) shows the contour made of a DEM dataset near Salt Lake City, Utah. Note the vertical lines which interrupt

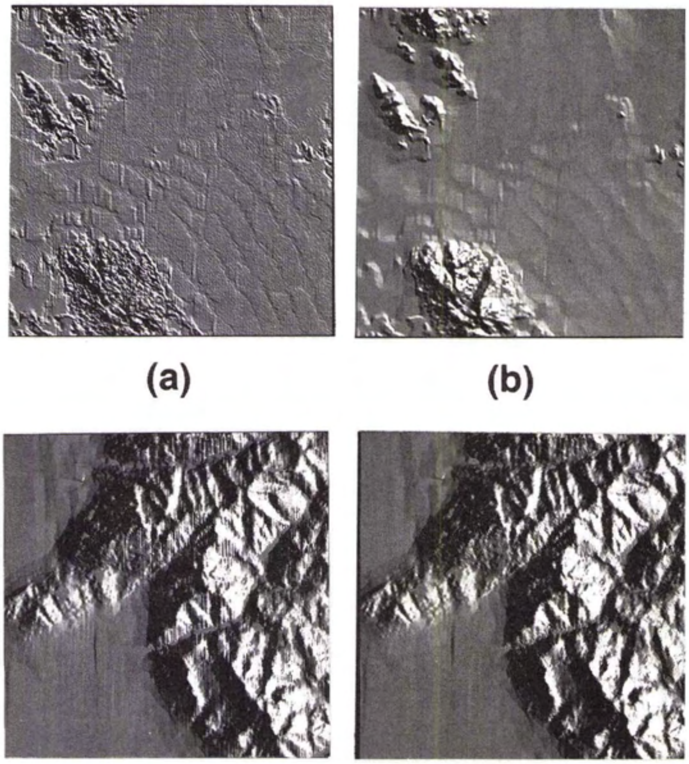

(a) (b) (c) (d)

FIG. 5. Shaded-relief images of DEM data. (a) DEM dataset in the area of Ft. Huachuca, Arizona, (b) Low-pass filtered DEM data of (a). (c) DEM dataset in the area of Salt Lake City, Utah. (d) Low-pass filtered DEM data of (c).

with the original data can be extracted using a high-pass wedge filter for wavelengths less than 360 metre and in the direction $-15° \leq \theta \leq °15$. Figure 4(d) shows the result of subtracting this output from the input data. The cutoff wavelength is estimated from the contour map of the DEM dataset. Using specified wavelengths to design filters is helpful to quantitatively interpret the topographic wavelengths of the filtered data.

Figure 5(a) is a shaded-relief image of the original DEM dataset in the area of Ft. Huachuca, Arizona. The artificial illumination was generated using a solar elevation angle 30° and an azimuth of 45° (northeast). Figure 5(b) is the filtered image derived using the same filter as in Figure 4(b). The significant difference is that ridges in the mountainous area can be identified in the filtered data, but are difficult to recognize in the original data.

Figure 5(c) is a shaded-relief image generated from the original DEM dataset in the area of Salt Lake City, Utah. The solar elevation angle is 30° and the azimuth is 90° (east). Figure 5(d) is the filtered image using the same filter as in Figure 4(d). Most of vertical line-type noise corrupted with the DEM dataset are no longer evident.

The filtering technique cannot remove all random noise perfectly, but does provide an analytic approach to control the retrieved signal with specified wavelengths and directions. The filter toolbox provides an efficient way to examine various digital spatial data.

DISCUSSION

The functions of a filter toolbox have been discussed and examples of its use were demonstrated. The power spectrum is useful to identify noise resulting from different factors. The point filter can be used to remove periodic noise and the line filter can be used to handle line-type noise-related frequencies. Area filters, including high-pass, band-pass, low-pass, and wedge filters, are useful for general purpose filtering studies.

One mosaicking problem, which could arise from the application of the filtering techniques, results in situations where two adjacent filtered spatial datasets may not be continuous at the adjacent edge. One way to avoid this problem is to design a spatial filter, if it is possible, based on the specifications of the frequency responses, then multiply this spatial filter with the input dataset. The spatial filter must have a small kernel to reduce the computation time and minimize the edge effect. Several such kernels are under study and may be helpful in the filtering of large spatial datasets.

ACKNOWLEDGMENTS

The author appreciates Donald Orr, June Thormodsgard, Bruce Quirk, John Dwyer, and Joy Hood for their helpful reviews and contributions of image data.

REFERENCES

Bailey, G. B., J. L. Dwyer, and D. J. Meyer, 1988. AVIRIS data characteristics and their effects on spectral discrimination of rocks exposed in the drum mountains, Utah: results of a preliminary study. *Proceedings of AVIRIS Performance Evaluation Workshop*, Pasadena, California, June 1988, p. 13.

Bath, M., 1974. *Spectral Analysis in Geophysics*. Elsevier, Amsterdam, 563 p.

Bendat J. S., and A. G. Piersol, 1971. *Random Data: Analysis and Measurement Procedures*. Wiley Interscience, New York, 407 p.

Chen, C. F., K. J. Worrell, W. R. Bergan, and F. L. Scarpace, 1987. Application of frequency filtering in the remotely sensed imagery. *ASPRS-ASCM Technical Papers*, Vol. 6, pp. 98–107.

Cooley, J. W., and J. W. Turkey, 1965. An algorithm for the machine calculation of complex Fourier series. *Mathematics of Computation*, Vol. 19, pp. 297–301.

Dehlinger, P., 1978. *Marine Gravity*. Elsevier, New York, 322 p.

Hassan, M. M., 1988. Filtering digital profile observations. *Photogrammetric Engineering and Remote Sensing*, Vol. 54, No. 10 pp. 1391–1394.

Moik, J. G., 1980. *Digital Processing of Remotely Sensed Images*. NASA SP-431, Washington, D. D., 330 p.

Oppenheim, A. V., and Schafer, R. W., 1975. *Digital Signal Processing*. Prentice Hall, Englewood Cliffs, New Jersey, 585 p.

Spector, A., and Grant, F. S., 1970. Statistical models for interpreting aeromagnetic data. *Geophysics*. Vol. 35, pp. 293–302.